Biophysical Journal Volume 68 June 1995 2588–2600

Photobleaching Kinetics of Fluorescein in Quantitative Fluorescence Microscopy

Loling Song,*‡ E. J. Hennink,*§ I. Ted Young,‡ and Hans J. Tanke*

*Department of Cytochemistry and Cytometry, Faculty of Medicine, Leiden University, 2333 AL Leiden; ‡Department of Pattern Recognition, Faculty of Applied Physics, Delft University of Technology, 2628 CJ Delft; and §Lambert Instruments, 9313 TH Leutingewolde, The Netherlands

ABSTRACT An investigation on the photobleaching behavior of fluorescein in microscopy was carried out through a systematic analysis of photobleaching mechanisms. The individual photochemical reactions of fluorescein were incorporated into a theoretical analysis and mathematical simulation to study the photochemical processes leading to photobleaching of fluorescein in microscopy. The photobleaching behavior of free and bound fluorescein has also been investigated by experimental means. Both the theoretical simulation and experimental data show that photobleaching of fluorescein in microscopy is, in general, not a single-exponential process. The simulation suggests that the non-single-exponential behavior is caused by the oxygen-independent, proximity-induced triplet-triplet or triplet-ground state dye reactions of bound fluorescein in microscopy. The single-exponential process is a special case of photobleaching behavior when the reactions between the triplet dye and molecular oxygen are dominant.

INTRODUCTION

Photobleaching is a dynamic process in which fluorochrome molecules undergo photo-induced chemical destruction upon exposure to excitation light and thus lose their ability to fluoresce. The photobleaching phenomenon has been the basis of many fluorescence measurement techniques developed and successfully applied since the 1970s. One of the most widely known is fluorescence photobleaching recovery (FPR) based on early work by Peters et al. (1974). Much of the essentials of current FPR has come from the laboratories of W. W. Webb and E. L. Elson (Axelrod et al., 1976; Edidin et al., 1976; Jacobson et al., 1976; Schlessinger et al., 1976, 1977). FPR, with its variants known as fluorescence redistribution after photobleaching (Koppel et al., 1986) and fluorescence microphotolysis (Peters et al., 1981), has been widely used in the past 20 years to study the rates of diffusion of fluorescent molecules inside and on the surface of cells. In the area of fluorescence resonance energy transfer, Jovin and others have applied photobleaching to derive the efficiency of energy transfer between a fluorescent donor and an acceptor molecule in microscopy (Jovin and Arndt-Jovin, 1989; Jovin et al., 1990; Kubitscheck et al., 1991, 1993; Marriott et al., 1991; Szabò et al., 1992; Young et al., 1994). This method offers the distinct advantage that complex corrections associated with the determination of energy transfer by combined donor and sensitized acceptor emissions are avoided. The approach is based on the demonstration of Hirschfeld (1976) that, for unimolecular or pseudo-unimolecular reactions, the time-integrated emission of a single-exponential photobleaching process is independent of fluorophore quantum yield, excitation intensity, and photobleaching lifetime. Kubitscheck et al. (1991) also tried to accommodate more complex decay kinetics.

The development of the abovementioned techniques made it possible to derive quantitative measurements in various applications in cell science. However, the mechanisms of photobleaching in biological objects are not yet well understood (for review see Tsien and Waggoner, 1989; Wells et al., 1989). Almost all the existing knowledge on photobleaching comes from spectroscopy studies of fluorochrome molecules in solution. In spectroscopy, free fluorochrome molecules are homogeneously dissolved in solution, and the chemical environment is well controlled. A single phenomenon is studied at a time and generally single-exponential bleaching is observed.

In microscopy, however, there have not been systematic studies on the mechanisms of photobleaching. It is generally assumed that the photobleaching analysis of fluorochrome in solution can be directly applied to the microscope situation. This assumption does not take into account that, in microscopy, fluorochrome molecules are chemically bound to targets of interest (such as DNA, RNA, protein, or other cellular components) about which the chemical microenvironment is very complex, often differs from one specimen to another, and is very difficult to control. Although a single-exponential (or first-order) process is often used as a basis for the photobleaching techniques in microscopy, the experimental data from many studies deviate from a pure single-exponential function $I = Be^{-kt}$ (Benson et al., 1985; Koppel et al., 1989; Rigaut and Vassy, 1991). Benson et al. (1985) carried out an extensive study on the heterogeneous photobleaching rates of different areas within a cell using various fluorochromes. They described their experimental bleaching curve by a three-parameter exponential: $I = A + Be^{-kt}$ for each pixel in an image, where the offset A was attributed to the ever-present background fluorescence. Koppel et al. (1989) used an identical model in their analysis of photobleaching.

Received for publication 31 October 1994 and in final form 19 March 1995.

Address reprint requests to Loling Song, Dept. of Cytochemistry and Cytometry, Leiden University, Wassenaarseweg 72, 2333 AL Leiden, The Netherlands. Tel.: 31-71-276198; Fax: 31-71-276180; E-mail: loling@ruly46.leidenuniv.nl.

0006-3495/95/06/2588/13 $2.00

Rigaut and Vassy (1991) examined their photobleaching curve by transformation in log (i.e., single exponential without an offset) and demonstrated that photobleaching in confocal microscopy was clearly not a single-exponential process, but the origin of the non-single-exponential behavior was not discussed. Szabò et al. (1992) reported in their study using photobleaching fluorescence resonance energy transfer that the photobleaching kinetics of FITC (fluorescein isothiocyanate) attached to immunoglobulin followed a double-exponential process. In their analysis for the possible explanation of the second exponential component, they speculated that the difference in accessibility of quencher molecules to the fluorochrome molecules and the photochemical destruction of the triplet FITC molecules could be among the reasons for the double-exponential behavior.

The experimental deviation from the single-exponential behavior, as repeatedly observed by different research groups, is not likely to be accidental. This leads to a fundamental question of whether certain photochemical processes could give rise to non-single-exponential photobleaching behavior under microscope conditions. A better understanding of photobleaching in microscopy will allow further utilization of this phenomenon, which is of particular interest in quantitative analysis of fluorescently stained tissues, cells and cell organelles using confocal laser scanning microscopy or digital imaging microscopy (see Carrington et al. (1989) and Tsien and Waggoner (1989) for review).

The study reported here is aimed at a systematic analysis of photobleaching kinetics in microscopy. It focuses on the photobleaching process of fluorescein alone. First, the photochemical and photophysical background of photobleaching is discussed with a detailed analysis focusing on the specific mechanisms applicable to fluorescein. Then, new experiments on the photobleaching characteristics of free fluorescein in solution and of fluorescein covalently attached to nucleic acid probes in microscopy are presented. Through a mathematical simulation, photochemical knowledge of fluorescein from earlier studies (Lindqvist, 1960; Kasche and Lindqvist, 1964; Usui et al., 1965) is used to study the kinetics of fluorescein from a theoretical point of view. The results from the simulation are compared with the experimental data. Finally, the effects of different photobleaching mechanisms on the behavior of the photobleaching process of fluorescein are discussed. It is demonstrated theoretically and experimentally that the photobleaching of fluorescein in microscopy is, in general, not a single-exponential process.

PHOTOCHEMICAL AND PHOTOPHYSICAL BACKGROUND

Decay and photobleaching

Decay and photobleaching are two distinct light-induced processes, taking place on very different time scales. Upon exposure to excitation light with irradiance H (W cm^{-2}) and wavelength λ_{ex} (m), fluorochrome molecules absorb the photon energy (hc/λ_{ex}, with Planck's constant h, the speed of light c) and make an electronic transition from the low energy ground state S to the higher energy excited singlet state S*. The rate of photon absorption k_a (s^{-1}) by a fluorophore molecule with an absorption cross-section σ_a (cm^2 molecule^{-1}) is directly proportional to the photon flux and thus the irradiance according to

$$k_a = \sigma_a [H \cdot \lambda_{ex}/(hc)] \quad (1)$$

For fluorescein, σ_a is 3.06×10^{-16} cm^2/molecule at 488 nm and pH > 7 (Tsien and Waggoner, 1989). With pulsed excitation, the number of fluorophore molecules that absorb the photon energy and reach the excited singlet state will attain a certain maximum, and then become depopulated via fluorescence emission, radiationless internal conversion, and radiationless intersystem crossing to the excited triplet state T*, at rates k_f, k_{ic}, and k_{isc}, respectively (Fig. 1). Decay refers to the composite effect of these three processes after the fluorophore is exposed to a narrow pulse of excitation light. The decay lifetime, S*, of a fluorophore is the inverse of the sum of these three rate constants and rate constants of any other processes (e. g., resonance energy transfer), which depopulate S*. Namely,

$$\tau_{s*}^{-1} = \sum k = k_f + k_{ic} + k_{isc} + \ldots + k_{other}$$

and it is commonly 1–10 ns. The decay lifetime is intrinsic to a particular fluorophore, and thus independent of excitation intensity for levels below saturation. Molecules that cross to the excited triplet state are likely to be trapped in that state for a duration of microseconds to milliseconds, since the T*→S transition is spin-forbidden and therefore the rate k_l of the T*→S transition is very low. The decay process does not necessarily involve fluorophore decomposition, although the latter could take place.

In contrast, photobleaching is the process in which the total number of ground state molecules is depleted via per-

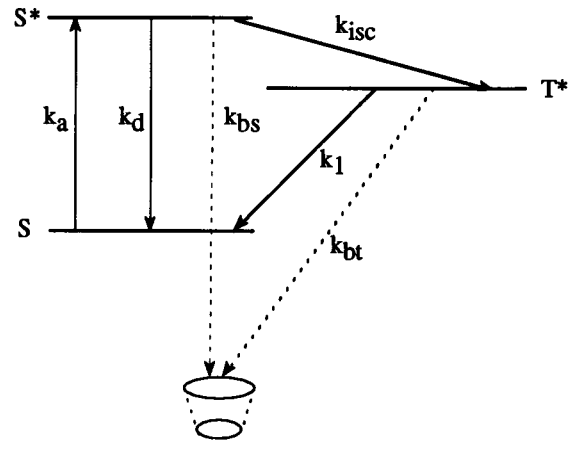

FIGURE 1 Simplified Jablonski energy diagram for a generic fluorochrome. S, S*, and T* represent ground singlet, excited singlet, and excited triplet electronic energy levels, respectively. Fluorochrome molecules absorb photon energy at a rate k_a and go from the ground singlet state S up to the excited singlet state S*. Then they may return to the ground state by radiative (fluorescence) or non-radiative (internal conversion) pathway at a combined rate k_d. They may also undergo non-radiative intersystem crossing, at a rate k_{isc}, to T*, where they may return to the ground state at a rate k_l. Photobleaching may take place from both S* and T* at rates k_{bs} and k_{ts}, respectively. Those photobleached molecules can no longer participate in the excitation-emission cycle.

manent photochemical destruction when molecules are either in the singlet or the triplet excited state. Photobleaching is the cumulative effect of fluorophore loss from each excitation-emission cycle over time, and the rate of photobleaching is a function of the excitation intensity. Those bleached molecules can no longer participate in the excitation-emission cycle. Under normal mercury arc lamps, photobleaching is observed on the time scale of seconds to minutes. With a laser as an excitation source, photobleaching can occur in as short as a few microseconds. Fig. 2 depicts the conceptual difference between decay and photobleaching processes.

For an "ideal" case in the absence of photobleaching, the population kinetics of each energy state are described by:

$$\frac{d}{dt}[N_S(t)] = -k_a N_S(t) + k_d N_{S^*}(t) + k_1 N_{T^*}(t)$$

$$\frac{d}{dt}[N_{S^*}(t)] = k_a N_S(t) - (k_d + k_{isc}) N_{S^*}(t) \qquad (2)$$

$$\frac{d}{dt}[N_{T^*}(t)] = k_{isc} N_{S^*}(t) - k_1 N_{T^*}(t)$$

where $N(t)$ is the molecular population in the energy state designated by the subscript as a function of time, and k_d is the sum of k_f and k_{ic}. Shortly after exposure to a constant excitation light intensity, the population in the singlet excited state establishes a steady state. For longer times, the triplet state also achieves a steady state ($(d/dt)[N_S(t)] \equiv (d/dt)[N_{S^*}(t)] \equiv (d/dt)[N_{T^*}(t)] = 0$). The system in Eq. 2 can then be solved for N_S, N_{S^*}, and N_{T^*}, with the normalized constraint $N_S(t) + N_{S^*}(t) + N_{T^*}(t) = 1$:

$$N_{S^*} = \frac{k_a k_1}{k_1(k_a + k_d + k_{isc}) + k_a k_{isc}}$$

$$N_{T^*} = \frac{k_a k_{isc}}{k_1(k_a + k_d + k_{isc}) + k_a k_{isc}}$$

$$N_S = 1 - N_{S^*} - N_{T^*} = 1 - \frac{k_a(k_1 + k_{isc})}{k_1(k_a + k_d + k_{isc}) + k_a k_{isc}}.$$

All the dye molecules are assumed to reside in the ground state before the onset of the excitation and are normalized to unity. The steady state is maintained, and the population in each state is part of the total initial population in the ground state. The relative number of molecules in each state is a function of the excitation rate. At low excitation rate ($k_a \ll k_d$) and at constant k_1 and k_{isc}, N_{S^*} and N_{T^*} are small fractions, and $N_S \rightarrow 1$, i.e., most of the molecules, reside in S ($N_S \gg N_{S^*}, N_{T^*}$). At high excitation rate ($k_a > k_d$), N_S is less than both N_{S^*} and N_{T^*}, and most of the molecules are continuously pumped up to S*, from which they cross to T* at a rate k_{isc}. For any excitation rate, if $k_1 \ll k_{isc}$, over time $N_T \gg N_{S^*}$, and a large number of molecules accumulate in the lowest triplet excited state.

In practice, however, photobleaching does take place, and fluorophore molecules undergo permanent photochemical destruction while they are in the excited singlet or triplet state. The steady state no longer holds [$(d/dt)[N_S(t)] \neq 0$; $(d/dt)[N_{S^*}(t)] \neq 0$; $(d/dt)[N_{T^*}(t)] \neq 0$.]. Instead, within a time period governed by the rates of all the reactions involved, the populations of the ground state, excited singlet, and excited triplet states will change in unison according to a characteristic function determined by the reactions involved in the photochemical destruction. Hirschfeld (1976) derived an analytical expression where photobleaching is assumed to take place from the excited singlet state and the photochemical reactions are of a unimolecular or pseudo-unimolecular nature. He demonstrated that photobleaching followed a single-exponential function. Wells et al. (1989) derived an analytical expression for photobleaching from the excited triplet state. In both of these analyses, the models were simplified to a single (combined) unimolecular or pseudo-unimolecular photochemical reaction. In microscopy, the photochemical reactions are much more complex, sensitive to various environmental factors, and can involve many bimolecular processes. In the following section, a detailed analysis will be carried out for fluorescein photobleaching in microscopy.

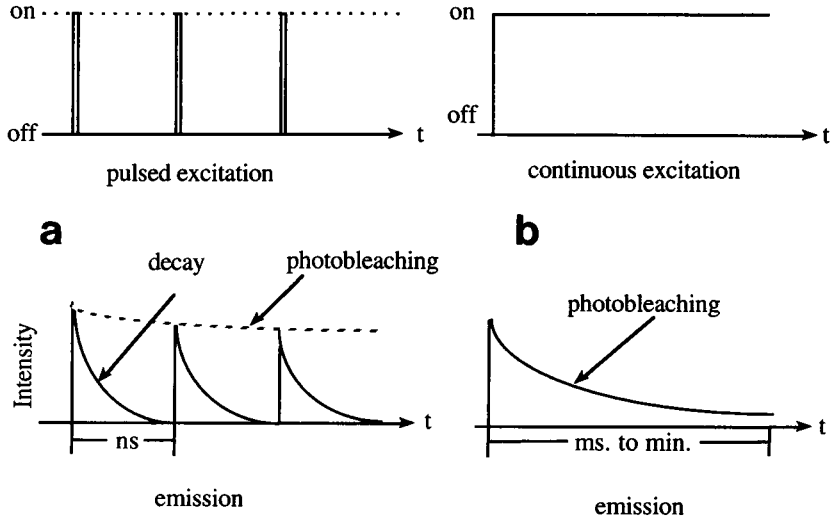

FIGURE 2 Schematic diagram depicting the conceptual difference between the decay and photobleaching processes. The diagrams above are the types of excitation, pulsed or continuous, and those below are the corresponding emission. (*a*) Decay refers to the depopulation of the excited singlet state after experiencing a brief excitation pulse. This process does not necessarily involve a permanent loss of fluorochrome molecules, although the latter often occurs. The decay process can be resolved on the time scale of nanoseconds. (*b*) Photobleaching is a process in which the total amount of ground state molecules are depleted via permanent photochemical destruction. Photobleaching is the cumulative effect of fluorophore loss from each excitation-emission cycle due to a continuous exposure to the excitation light. Photobleaching in fluorescence microscopy can be observed on the time scale of microseconds to minutes.

Photochemical properties and photobleaching mechanisms of fluorescein

Although in principle bimolecular processes between a singlet excited state dye molecule and a molecule of another species (such as oxygen) can lead to photobleaching from the dye singlet, there has not been much evidence of this phenomenon for fluorescein so far. In the early 1960s, Lindqvist conducted an extensive flash photolysis study on the photoreactions of fluorescein in deaerated water (Lindqvist, 1960). This was followed by studies on the reactions of triplet fluorescein with oxygen (Kasche and Lindqvist, 1964). Lindqvist pointed out that because of its very short decay lifetime (4.5 ns) in aqueous solution, the singlet excited state was not ordinarily responsible for the photochemical activity of fluorescein. Imamura and Koizumi (1955) showed, through a theoretical estimation based on oxygen diffusion in aqueous solution, that the lifetime of the intermediate to be attacked by oxygen must be at least 10^{-6} s. More recently, Gollnick et al. (1992) found that oxygen exerted no measurable effect on the short-lived excited singlet state of xanthene dyes even in oxygen-saturated solutions. There was, however, much evidence in these studies for the existence of quenching of the long-lived lowest triplet excited state, which was populated exclusively by a transition from the singlet excited state. Lindqvist (1960) demonstrated that the triplet excited state fluorescein molecules became depopulated via two major pathways: one was the reaction between a triplet and another triplet or a ground state dye molecule; and the other was the reaction between a triplet dye molecule and an oxygen molecule. These two mechanisms were later studied by Usui et al. (1965) and called D-D (dye-to-dye) and D-O (dye-to-oxygen) mechanisms, respectively. The major reactions involved in these two mechanisms are listed in Table 1, along with the corresponding rate constants derived by Lindqvist for the pH range used in the present study. Reactions 4 ($T^* + T^* \rightarrow R + X$) and 5 ($T^* + S \rightarrow R + X$) represent the occurrence of an electron transfer process, which leads to the formation of semi-reduced (R) and semi-oxidized (X) radical forms of the dye molecule. These radicals in turn undergo further reaction(s) reverting either to the ground state dye (Krüger and Memming, 1974) or to stable non-fluorescent photoproduct(s). The exact fate of these radicals was difficult to determine in Lindqvist's (1960) study. In the present study, all X and R molecules are considered candidates for the bleached dye molecules. It is noteworthy that the electron transfer processes (reactions 4 and 5) compete with the two quenching processes (reaction 2, $T^* + T^* \rightarrow T + S$, and reaction 3, $T^* + S \rightarrow S + S$) respectively with about equal efficiency. Quenching of T^* by X and R (respectively, $T^* + X \rightarrow S + X$ and $T + R \rightarrow S + R$) leads to the return of T^* back to S at an equal rate without causing a net population change in X and R. Quenching of T^* by O_2 leads to physical quenching ($T^* + O_2 \rightarrow S + O_2$) at a rate of about one order of magnitude faster than the chemical quenching ($T^* + O_2 \rightarrow X + HO_2$).

To study the photobleaching behavior of fluorescein, all of the photochemical reactions from the studies of Lindqvist and Kasche (Lindqvist, 1960; Kasche and Lindqvist, 1964) are incorporated into a model described by the following six coupled differential equations:

$$\begin{aligned}
\frac{d}{dt}[N_S(t)] &= [k_d N_{S^*}(t) + k_1 N_{T^*}(t) + k_2 N_{T^*}^2(t) \\
&\quad + k_3 N_{T^*}(t) N_S(t) + k_6 N_{T^*}(t) N_X(t) + k_7 N_{T^*}(t) N_R(t) \\
&\quad + k_8 N_{T^*}(t) N_{O_2}(t)] - [k_a N_S(t) + k_5 N_{T^*}(t) N_S(t)] \\
\frac{d}{dt}[N_{S^*}(t)] &= k_a N_S(t) - [k_d N_{S^*}(t) + k_{isc} N_{S^*}(t)] \\
\frac{d}{dt}[N_{T^*}(t)] &= k_{isc} N_{S^*}(t) - [k_1 N_{T^*}(t) + k_2 N_{T^*}^2(t) \\
&\quad + k_3 N_{T^*}(t) N_S(t) + 2k_4 N_{T^*}^2(t) + k_5 N_{T^*}(t) N_S(t) \\
&\quad + k_6 N_{T^*}(t) N_X(t) + k_7 N_{T^*}(t) N_R(t) + k_8 N_{T^*}(t) N_{O_2}(t) \\
&\quad + k_9 N_{T^*}(t) N_{O_2}(t)] \\
\frac{d}{dt}[N_X(t)] &= k_4 N_{T^*}^2(t) + k_5 N_{T^*}(t) N_S(t) + k_9 N_{T^*}(t) N_{O_2}(t) \\
\frac{d}{dt}[N_R(t)] &= k_4 N_{T^*}^2(t) + k_5 N_{T^*}(t) N_S(t) \\
\frac{d}{dt}[N_{O_2}(t)] &= -k_9 N_{T^*}(t) N_{O_2}(t).
\end{aligned} \tag{3}$$

In this system, k_1–k_9 are those derived by Lindqvist and Kasche (Lindqvist, 1960; Kasche and Lindqvist, 1964) for the pH range in the current study (Table 1). The nonlinearity introduced by the bimolecular processes makes it extremely difficult to find an analytical solution for the system in Eq. 3. Instead, an efficient iterative numerical method has to be used to study the photobleaching kinetics of fluorescein.

MATERIALS AND METHODS

Experimental approach

Free fluorescein in solution

A fluorescein solution of 0.01 μM was made by dissolving fluorescein sodium (Merck's certified grade, without further purification) in phosphate-buffered saline (PBS; pH 7.6). The solution was then placed in three cuvettes: 1) control sample, which was not exposed to the bleaching light source, 2) air-saturated sample, and 3) deoxygenated sample, from which oxygen was purged by flushing argon gas (oxygen content < 0.5 ppm, Hoekloos BV, Schiedam, The Netherlands) for 15 min. A Leitz DM epi-fluorescence microscope (Leica, Wetzlar, Germany) with a 100-W mercury arc lamp and a 450–490-nm excitation filter block was used as a bleaching light source. The objective lens was removed so that a column of light was impinged on the cuvette. The air-saturated and argon-flushed samples were exposed to the continuous bleaching light source for 90 min. The fluorescence intensity was measured before the first exposure and again at 15-min intervals on a spectrofluorometer (SPF-500, SLM Instruments, Inc., Urbana, IL). The cuvettes were well shaken before each measurement. The spectrofluorometer was equipped with a xenon lamp, and the emission and ex-

TABLE 1 Photochemical reactions of fluorescein

Reaction	No.	Description	Rate constants‡
$S + h\nu \rightarrow S^*$		Absorption	$k_a = 3.8 \times 10^8\ s^{-1}$
$S^* \rightarrow S + h\nu'$		Fluorescence emission	$k_d = 2.134 \times 10^8\ s^{-1}$
$S^* \rightarrow S$		Internal conversion	
$S^* \rightarrow T^*$		Intersystem crossing	$k_{isc} = 6.6 \times 10^6\ s^{-1}$
$T^* \rightarrow S$	1	Radiationless deactivation	$k_1 = 50\ s^{-1}$
$T^* + T^* \rightarrow T^* + S$	2	Triplet quenching	$k_2 = 5 \times 10^8\ M^{-1}\ s^{-1}$
$T^* + S \rightarrow S + S$	3		$k_3 = 5 \times 10^7\ M^{-1}\ s^{-1}$
$T^* + T^* \rightarrow R + X$	4	Electron transfer	$k_4 = 6 \times 10^8\ M^{-1}\ s^{-1}$
$T^* + S \rightarrow R + X$	5	Electron transfer	$k_5 = 5 \times 10^7\ M^{-1}\ s^{-1}$
$T^* + X \rightarrow S + X$	6	T* quenching by X	$k_6 + k_7 = 1 \times 10^9\ M^{-1}\ s^{-1}$
$T^* + R \rightarrow S + R$	7	T* quenching by R	k_7
$T^* + O_2 \rightarrow S + O_2$	8	Physical quenching by O_2	$k_8 = 1.56 \times 10^9\ M^{-1}\ s^{-1}$
$T^* + O_2 \rightarrow X + HO_2$ (or O_2^-)	9	Chemical quenching by O_2	$k_9 = 1.4 \times 10^8\ M^{-1}\ s^{-1}$

S, ground state dye; S*, singlet excited state dye; T*, triplet excited state dye; R, semi-reduced form of the dye; X, semi-oxidized form of the dye; O_2, oxygen.
‡The rate constants K_1 to K_9 were quoted from Lindqvist (1960) and Kasche and Lindqvist (1964), and k_a, k_d and k_{isc} were quoted from Tsien and Waggoner (1989).

citation monochromator slits were set to 490 ± 4 nm and to 512 ± 4 nm, respectively. All the instrument settings were kept constant throughout the experiment.

Bound fluorescein in microscopy

Fluorescein surface-labeled microspheres (Quantum Series 25, Flow Cytometry Standards Corp., Research Triangle Park, NC), suspended at a proper concentration in PBS, were centrifuged at 1200 × *g* for 30 min onto standard microscope slides. Non-adherent microspheres were gently rinsed off with PBS. The slides were air-dried in the dark and embedded in PBS in the absence of anti-fading agents.

Ficol-isolated human lymphocytes on glass slides were in situ hybridized and fluorescein molecules were directly (without antigen-antibody complex or spacer molecules) attached to probes specific for the centromeric region of chromosome 1. After in situ hybridization the preparation was counterstained with diamidino phenylindole and embedded under a coverslip in PBS.

The imaging system consisted of a Leitz Aristoplan fluorescence microscope equipped with a 100-W mercury arc lamp and a charge-coupled device (CCD) camera (series CH250, Photometrics Inc., Tucson, AZ) with a Kodak (Rochester, NY) KAF-1400 chip of 1348 lines × 1035 pixels by 12-bit planes. The shutter in the CCD camera and a mechanical shutter in the excitation light path were computer controlled for the desired on-chip integration and duration of illumination, respectively. A filter block with an excitation bandwidth of 450–490 nm, a dichroic mirror of 510 nm, and a long pass emission filter of 520 nm were used for fluorescein-stained specimens.

A Macintosh IIfx computer served as a host computer, which directly controlled the shutters and image acquisition. For each object of interest, a series of images were acquired over time under continuous steady illumination. For interphase chromosomes, a sequence of images were continuously acquired over a period of 120 s, and each image was integrated for 1.0 s. For fluorescent microspheres, images were also continuously acquired with an integration time of 0.7 s/image. For both preparations, a 2 × 2 binning on the CCD camera was used to increase the signal-to-noise ratio. The microscope was adjusted to Köhler illumination and checked for flat-field with uranyl glass. For background subtraction, the part of the gray value intensity image, $I(x,y,t)$, outside the area of the object was used. The background mask was found by first applying a gradient filter to $I(x,y,t = 0)$ and then thresholding the resultant image to locate the area with the magnitude of the gradient close to zero (i.e., the background area). This area was then used as an image mask for the subsequent images in the same series, and a mean value for each gray value intensity image under the background mask multiplied by the area of the whole image was subtracted from the total integrated intensity. The final scalar value of each image was the total integrated intensity after the background correction. A bleaching curve was formed by plotting intensity values of all the images in the series against time.

Theoretical approach

Study of kinetics by mathematical simulation

Based on the photochemical reactions and their rate constants derived from Lindqvist's studies (Lindqvist, 1960; Kasche and Lindqvist, 1964), a system of ordinary differential equations (ODEs) can be formulated from the reaction scheme (see Table 1 and Eq. 3). Each differential equation describes the change of a population of molecules over time. The kinetics can be monitored by solving this system of ODEs using numerical methods and integrating it from the nanosecond to the minute scale. The numerical methods made use of the highly efficient FORTRAN software package Livermore Solver for Ordinary Differential Equations (Hindmarsh, 1983) and was customized for the current study. The algorithm and the initial step size (Press et al., 1992) took into consideration the drastically different time scales originating from the nanosecond singlet excited state lifetime and micro- to millisecond triplet state lifetime (a so-called stiff problem). A strategy of a dynamically adjusted step size was used to ensure an accurate solution at the early (fast reaction) stage and a fast convergence of the solution at the later (slow reaction) stage of the photobleaching process. All computations were performed in double-precision.

Simulation of "free fluorescein in solution"

Simulation of the photobleaching process of free fluorescein in solution was accomplished by setting the appropriate initial conditions and recording the population change of each energy state over time. The initial conditions for simulation of air-saturated fluorescein in aqueous solution were $N_s(t = 0) = 0.01\ \mu M$ (as used in the Experimental Approach), and $N_{O_2}(t = 0) = 250\ \mu M$ (Usui et al., 1965). For simulation of the argon-flushed treatment, 0.01% of N_{O_2} of the air-saturated solution was used as an estimate based on the result of Vaughan and Weber (1970) that the inert gas flushing method did not completely remove all O_2. Then $N_{O_2} = 0.025\ \mu M$ and $N_s = 0.01\ \mu M$. In the cuvette experiment, in which the microscope objective was removed and collimated light was impinged upon the cuvette, the power density was much lower than that under the objective (see below). Then k_a was estimated to be ~0.038 s^{-1}. All the other rate constants (Table 1) used are intrinsic to fluorescein for the pH used in the present study, and were quoted directly from Lindqvist (Lindqvist, 1960; Kasche and Lindqvist, 1964).

Simulation of "bound fluorescein in microscopy"

When a fluorochrome is bound to a surface or encapsulated in a volume, the notion of concentration is no longer valid. An example would be fluorescein covalently bound to a nucleic acid sequence and tightly bound to a cellular target. To simulate this situation where the fluorochrome molecules can no longer diffuse freely, calibrated fluorescent beads from Flow Cytometry Standards Co. were used. These beads were 9 μm in diameter and densely coated with fluorescein equivalent to 2.0×10^6 soluble fluorochrome molecules on average (based on the manufacturer's definition). Assuming a homogeneous distribution of fluorochrome molecules over the bead surface, the average intermolecular distance would be comparable to that of a 10 mM fluorescein solution. Thus, for air-saturated aqueous embedding environment, the initial conditions used in the simulation are $N_{O_2} = 250$ μM and $N_s = 10$ mM.

The excitation irradiance under a 100-W Hg arc lamp, 63×/1.4 oil objective, and an excitation bandwidth of 450–490 nm, was measured by inserting an integrating sphere containing a silicon photodiode (Sensor Head Model 350, 3M Photodyne Inc., Camarillo, CA) under the objective lens. The power measured was converted, according to Eq. 1, to a k_a of ~ 38 s^{-1} for this microscope setup (see also Jovin et al., 1990). For confocal laser scanning fluorescence microscopy using 1 mW of 488 nm argon laser and an objective with 1.25 numerical aperture, k_a is 3.8×10^8 s^{-1} (Tsien and Waggoner, 1989).

RESULTS

Experimental result of free fluorescein in solution

The fluorescence intensity measured in the spectrofluorometer was plotted against time over the first 90 min of bleaching (Fig. 3). Purging oxygen by argon flushing reduced the photobleaching rate, but did not inhibit it completely. This indicated that photo-oxidation was not the only process that caused photobleaching. This experiment was repeated for a continuous argon flush throughout the 90-min period to rule out the possibility of O_2 leaking through the rubber stop and diffusing back into the solution. The result was the same as that of the single argon flush (data not shown). Both the air-saturated and argon-flushed bleaching rates were too slow for the extraction of a meaningful characteristic function.

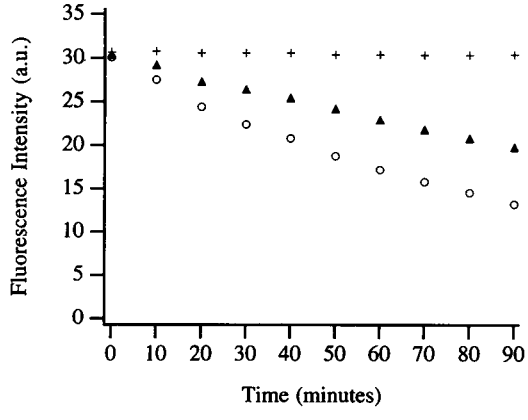

FIGURE 3 Effect of photobleaching on free fluorescein in solution. 0.01 μM fluorescein sodium/PBS (pH 7.6) was placed in three cuvettes: (+) dark control, not exposed to the bleaching light source; (▲) capped with a rubber stopper, argon flushed for 15 min, and exposed to the continuous bleaching light source; and (○) air saturated and exposed to the continuous bleaching light source. The fluorescence intensity was measured on a spectrofluorometer every 10 min over a period of 90 min.

Experimental result of bound fluorescein in microscopy

To ensure that the background correction did not introduce an offset to the bleaching curve and thereby cause a lack of compliance with a single-exponential function, a criterion was used such that the sum of the background pixel values after correction should be as close to zero as possible. With the method described in the earlier section, it was found that the sum of the background gray values after the correction was, on average, <1% of the total integrated intensity of the image.

Figs. 4 and 5 are two typical examples of bleaching curves derived from the bleaching time series of the images after background correction. The integrated intensity normalized by the maximum initial intensity was plotted against time. The non-random distribution of the least-square residuals indicated a deviation of the experimental data from a single-exponential function for both types of examples. This experiment was repeated for a large number of beads and fluorescently in situ hybridized chromosome centromeres in different embedding media and under different excitation intensities. In all cases, a behavior deviating from a single-exponential function was observed.

Simulation result of "free fluorescein in solution"

The initial conditions used in the simulation were selected so as to resemble closely the actual experimental conditions. Fig. 6 *a* shows the simulation result of the population kinetics of free fluorescein in air-saturated solution over a period of

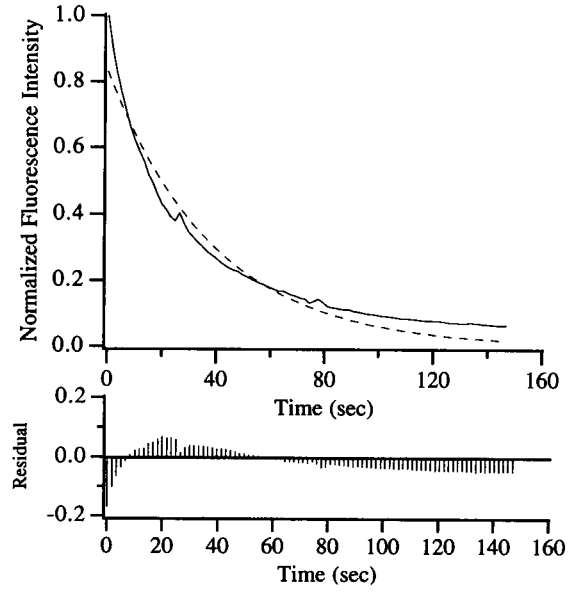

FIGURE 4 The photobleaching curve of a fluorescein surface-labeled microsphere. The microsphere was embedded in PBS (pH 7.6). The microscope setup was as described in the main text. The images were continuously acquired, and each image was integrated for 0.7 s. In the upper panel, the solid line represents the experimental data and the broken line represents the single-exponential fit. In the lower panel, the corresponding residual plot is shown.

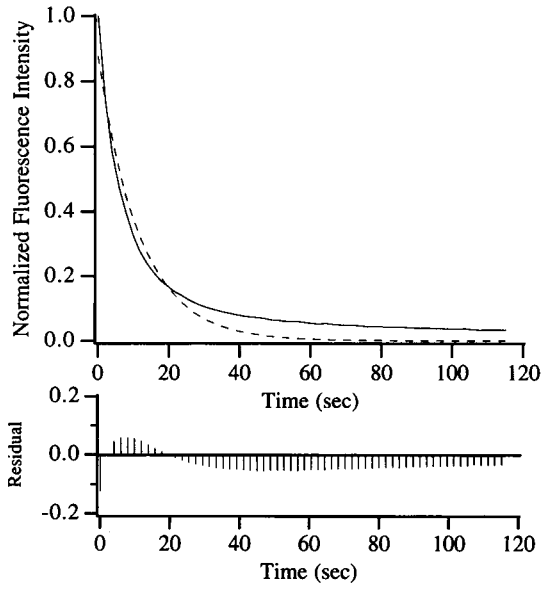

FIGURE 5 The photobleaching curve of the centromeric region of chromosome 1 in a human lymphocyte. The human lymphocytes were in situ hybridized and fluorescein was directly attached (without antibody-antigen complex or spacer molecules) to the probes specific for the centromeric region of chromosome 1. The interphase chromosomes were embedded in PBS (pH 7.6). The images were continuously acquired with an integration time of 1.0 s/image. For other imaging parameters, refer to the main text.

25 h. Because of the very low k_a (or the low irradiance of the bleaching light source), the ground state depletion could last many hours, and the majority of the dye molecules reside in S. The relative S* and T* populations were many orders of magnitude lower than S. However, the population of T* was greater than S* because of the accumulation over time, despite the low irradiance. The formation of X and R accompanied the depletion of S and was almost completely due to the D-O mechanism because of the high N_{O_2} (Fig. 6 *c*). The ground state depletion of the air-saturated fluorescein solution was completely described by a single-exponential function with the least-square residual very close to zero (Fig. 6 *b*). In the simulation of free fluorescein in the argon-flushed solution (Fig. 7, *a–c*) where $N_s/N_{O_2} = 0.4$, both D-O and D-D mechanisms operated, but the buildup of the bleached dye population was largely due to the D-O mechanism. Because of the participation of the D-D mechanism, the bleaching curve of the simulated argon-flushed fluorescein solution deviated slightly from a single-exponential function. Fig. 8 shows the comparison of the bleaching process for free fluorescein in air-saturated and argon-flushed solutions. The insert in Fig. 8 focuses on the first 90 min and demonstrates that the simulation very closely resembles the bleaching behavior observed in the actual experiment (Fig. 3).

Simulation result of "bound fluorescein in microscopy"

In the simulated conventional fluorescence microscopy case shown in Fig. 9, all the kinetic curves were normalized by the initial ground state population. The kinetic curve of the ground state depletion deviated significantly from a single-exponential function (Fig. 9 *a*). This confirms the experimental result in microscopy and indicates a non-single-exponential nature of the bleaching process. The buildup of the bleached dye population was predominantly due to the D-D mechanism with the D-O mechanism contributing a small portion (Fig. 9 *a*, *right*). If the D-D reactions were artificially suppressed (i.e., k_2, k_3, k_4, k_5, and k_6 were set to 0) while other parameters were held the same as in Fig. 9 *a*, then the kinetic curve of the ground state depletion could be completely described by a single-exponential function (Fig. 9 *b*). If the D-O reactions were artificially suppressed (i.e., k_8 and k_9 were set to 0) while other parameters were held the same as in Fig. 9 *a*, then the kinetic curve of the ground state depletion deviated from a single-exponential function (Fig. 9 *c*). If photobleaching was suppressed altogether (i.e., k_2, k_3, k_4, k_5, k_6, k_7, k_8, and k_9 were set to 0), then the populations of all three energy states came to a steady state equilibrium shortly after the onset of excitation (Fig. 9 *d*).

In the simulated confocal laser scanning microscopy, the high light intensity immediately "pumped" the ground state dye molecules to the excited triplet state (Fig. 10 *a*). The high triplet population greatly enhanced all the bimolecular processes involving T*, particularly reactions 4 and 5. The buildup of the bleached dye in this case (Fig. 10 *c*) was for the most part due to the D-D mechanism. Taking the log of the singlet excited state population resulted in a nonlinear curve indicating the deviation from a single-exponential function (Fig. 10 *b*).

DISCUSSION

Photobleaching via photooxidation (D-O) mechanism

Irreversible loss of fluorescence caused by the reaction between an oxygen molecule and a dye molecule has been the subject of numerous studies in photochemistry. It has also been recognized that photooxidation may not be the only process responsible for the irreversible loss of fluorescence. In the present study, purging oxygen by flushing the sample solution with argon only reduces the photobleaching rate. This result is consistent with the findings of Johnson et al. (1982). It indicates, on the one hand, that argon flushing may not completely remove all oxygen molecules and, on the other hand, that there may be at least one other bleaching process that is independent of oxygen.

It is interesting to note from Table 1 that, since the D-O mechanism consists of only one pseudo-unimolecular reaction (and thus one exponential term) leading to the bleached dye molecules, the bleaching behavior will be a single-exponential process in the absence of all D-D reactions. In the simulation of fluorescein in solution, where N_S is low and $N_S \ll N_{O_2}$, the probability of a reaction between dye molecules is very low. This probability is governed only by the concentrations of the reacting molecules, since the rate of reaction is constant at a given temperature. The photobleach-

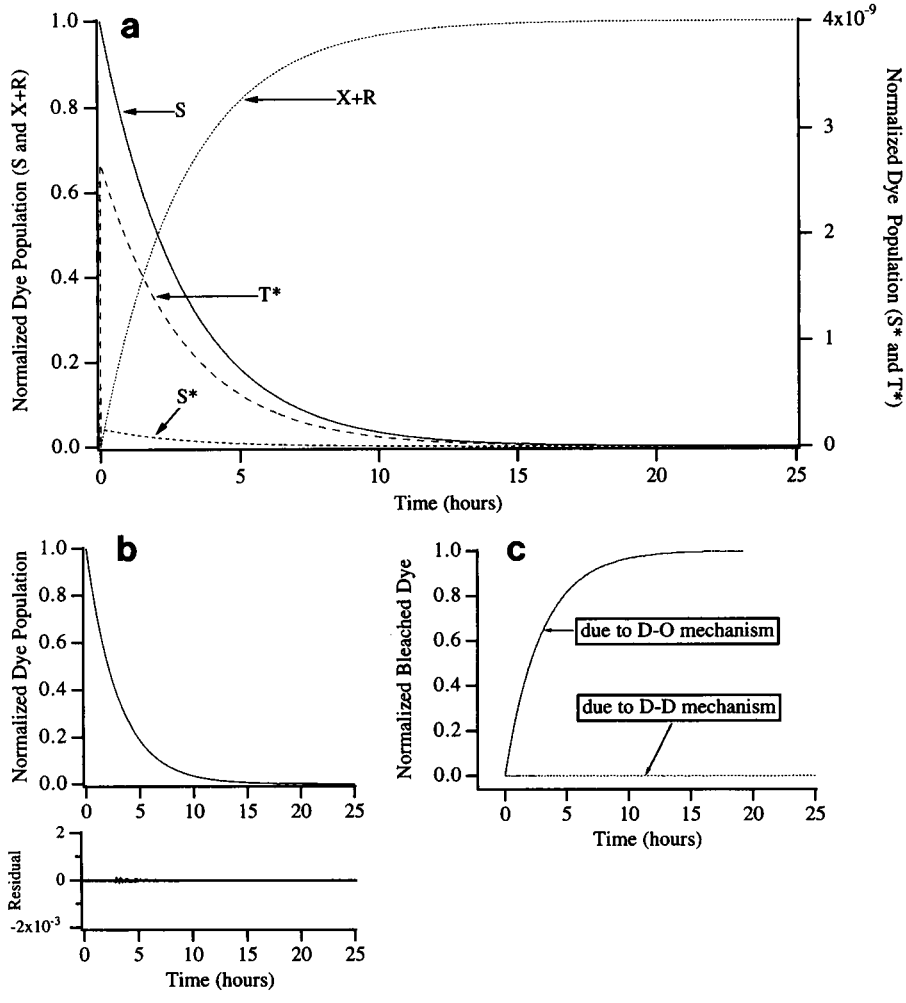

FIGURE 6 Simulation for free fluorescein in air-saturated solution. The parameters used for this simulation are: [F] = 0.01 μM, $[O_2]$ = 250 μM, k_a = 0.038 s^{-1}, and all other rate constants are as defined in Table 1. (*a*) population kinetic curves of fluorescein molecules in various energy states. S and X + R are plotted using the left vertical axis; S* and T* are plotted on another scale on the right. All populations are normalized by the initial dye population at the ground state, where all dye molecules are assumed to reside at t = 0. (*b*) Kinetic curve of the ground state depletion (———), the single-exponential fit (---) along with its least-square residual. (*c*) The formation of X and R due to different photobleaching mechanisms. Here the populations of X and R are grouped (added) together according to the reactions from which they are produced.

ing in this case is primarily caused by the D-O reactions and shows a single-exponential behavior (Fig. 6 *b*). In the simulation of bound fluorescein in microscopy, if the D-D reactions are assumed not to take part in photobleaching, then photobleaching is again a single-exponential behavior (Fig. 9 *b*) due solely to the D-O reactions. These simulation results suggest that single-exponential behavior is only a special case of photobleaching when D-O reactions are the predominant mechanism leading to photobleaching.

A thorough deoxygenation of the sample environment may not be completely advantageous with respect to the prevention of photobleaching. The complete removal of oxygen increases the triplet state lifetime (Tsien and Waggoner, 1989), increases the accumulation of triplet state dye molecules, and promotes the bimolecular reactions via the D-D mechanism. It is important to note that of the two reactions involving the D-O mechanism (physical quenching in reaction 8, $T^* + O_2 \rightarrow S + O_2$, and chemical quenching in reaction 9, $T^* + O_2 \rightarrow X + HO_2$ (Kasche and Lindqvist, 1964)), the physical quenching in fact does not lead to bleached molecules. Physical quenching enhances T*-S intersystem crossing and returns T* to S at a higher rate than chemical quenching converts T* to X. A complete removal of oxygen will inhibit physical quenching and thus fewer triplet state dye molecules are reverted back to the ground state to participate further in the excitation-emission cycle.

Photobleaching via D-D mechanism

Usui et al. (1965) provided evidence of a switchover between D-O and D-D mechanisms depending upon the relative concentrations of fluorescein ([F]) and of oxygen ($[O_2]$). It was concluded from their study that: 1) when [F] is very low and $[F] \ll [O_2]$ (i.e., $[F]/[O_2] < 0.2$), the D-O mechanism dominated, and the bleaching rate was simply proportional to the absorption of light; 2) when $[F] \gg [O_2]$ (i.e., $[F]/[O_2] > 0.2$), the D-D mechanism operated at a high rate, and the proportionality between the bleaching rate and the absorption of light no longer held.

The results of Usui et al. (1965) have an important implication for the present study. As stated earlier, in spectroscopy experiments, free fluorescein molecules are homogeneously distributed in air-saturated aqueous solution. At low concentration of fluorescein in air-saturated solution, $N_S \ll N_{O_2}$, and the reaction is dominated by D-O reactions. In microscopy, on the other hand, the situation is different in that fluorescein molecules are no longer freely diffus-

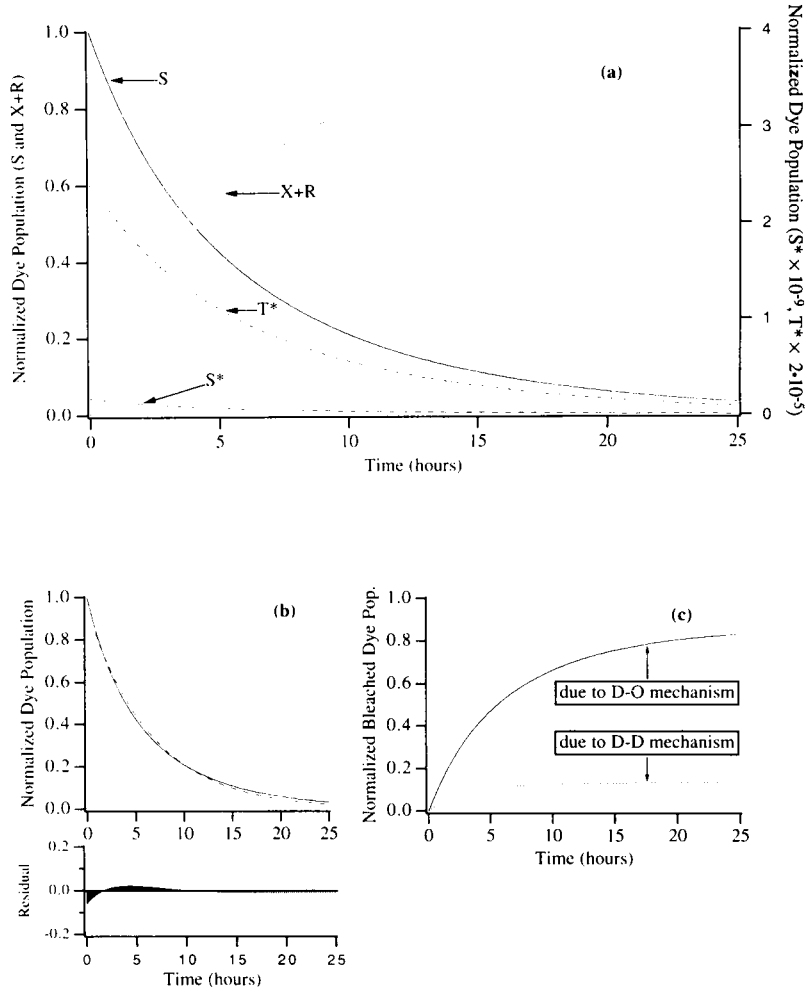

FIGURE 7 Simulation for free fluorescein in argon-flushed solution. The parameters used for this simulation were: [F] = 0.01 μM, $[O_2]$ = 0.025 μM, $k_a = 0.038\ s^{-1}$, and all other rate constants are as defined in Table 1. All populations are normalized by the initial dye population at the ground state. (*a*) Population kinetic curves of fluorescein molecules in various energy states. S and X + R are plotted using the left vertical axis; S* and T* are on another scale on the right axis. Note that T* is 4 orders of magnitude higher than S*. (*b*) Kinetic curve of ground state depletion (———), the single-exponential fit (---) and its least-square residual. (*c*) Formation of the bleached dye molecules due to D-D and D-O mechanisms.

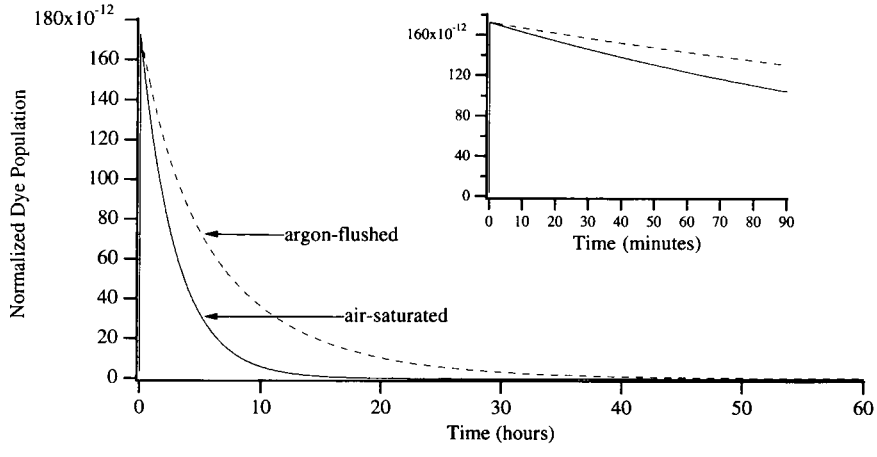

FIGURE 8 Comparison between the kinetic curves of the excited singlet population for free fluorescein in air-saturated and argon-flushed solutions. Each population is normalized by the initial ground state population. The parameters used for this simulation are as defined in the legends of Figs. 6 and 7. The insert shows the same curve during the first 90 min for the comparison with Fig. 3.

ible. The D-D reaction probability is a function of the intermolecular distance between the dye molecules. It is therefore conceivable that with [F] > $[O_2]$, the small intermolecular distance between the dye molecules (represented by a high initial [F]) promotes the proximity-induced D-D reactions. But as reactions proceed, the intermolecular distance between the dye molecules that can still react will become too large for D-D reactions. After that photobleaching will be dominated by D-O reactions.

The switching-over of the D-D and D-O mechanisms is observed in the current study, and the effects of each mechanism on the overall photobleaching behavior are also demonstrated. In the simulation of fluorescein

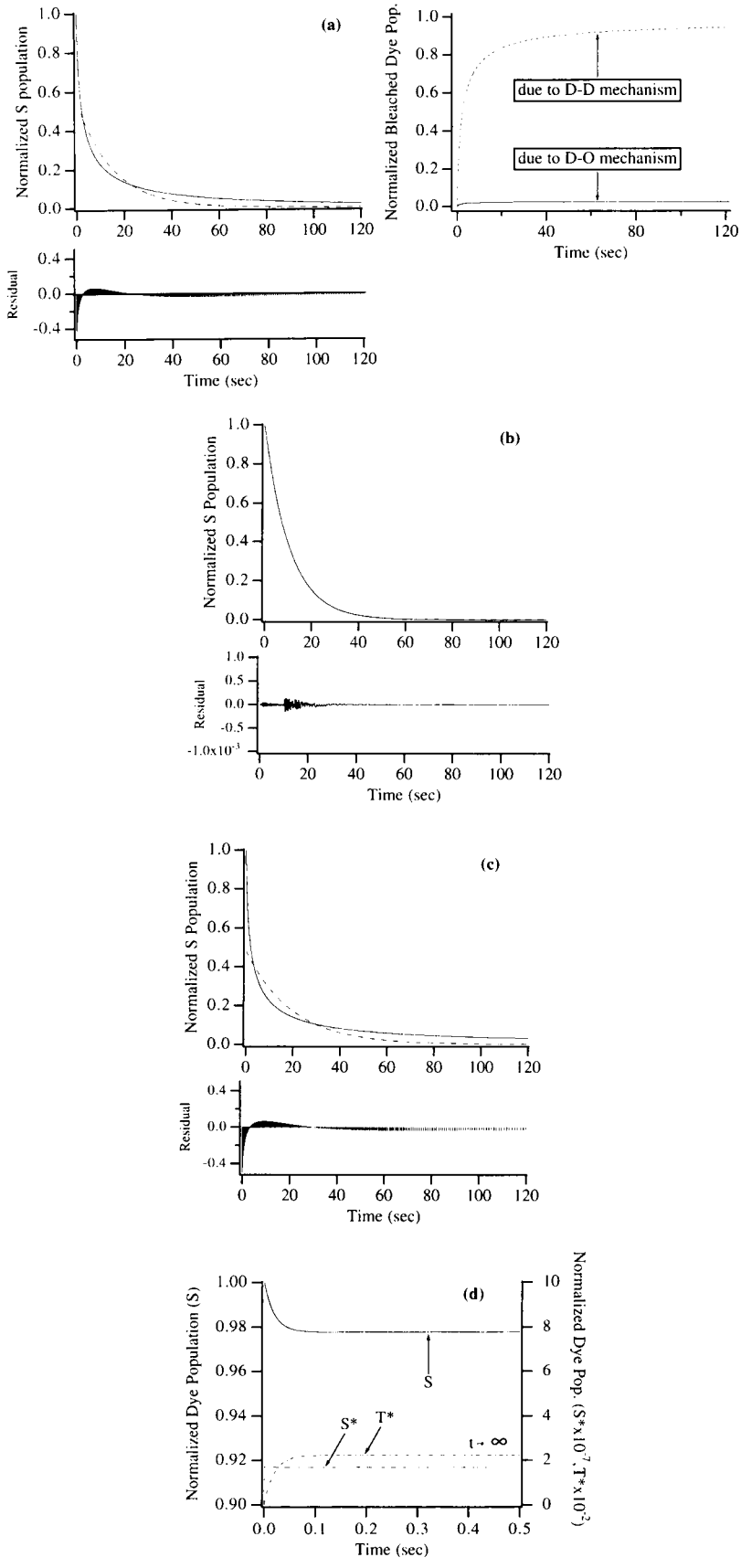

FIGURE 9 Simulation for bound fluorescein in conventional fluorescence microscopy. The parameters used for this simulation are: [F] = 10 mM, $[O_2]$ = 250 μM, k_a = 38 s^{-1}, and all other rate constants are as defined in Table 1. The high $[F]/[O_2]$ ratio is used to simulate the spatially close intermolecular distance among the dye molecules. (*a*) Kinetic curve of ground state depletion, and its residual (*left*) with the solid line representing the simulated data and the broken line the single exponential fit; formation of X and R due to different bleaching mechanisms (*right*). (*b*) Ground state kinetics when the D-D reactions are artificially suppressed and other parameters remain the same as in *a*. The simulated data and the singlet exponential fit overlap and the residual is very small. (*c*) Ground state kinetics when the D-O reactions are artificially suppressed and other parameters remain the same as in *a*. (*d*) Simulation of an "ideal" case of no bleaching, where both D-O and D-D reactions are artificially suppressed.

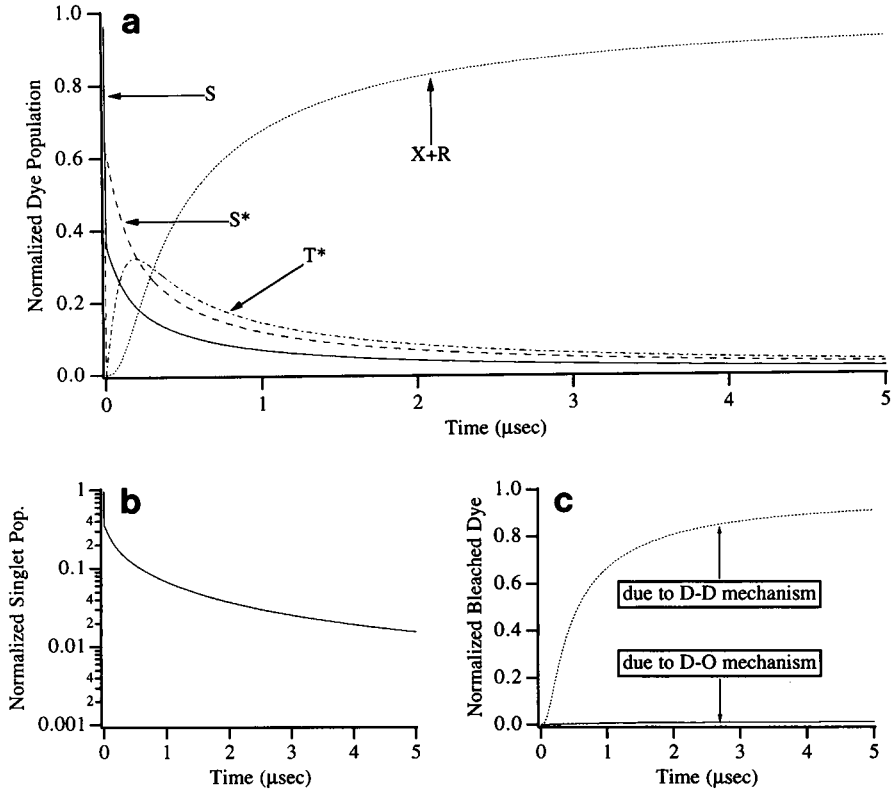

FIGURE 10 Simulation for bound fluorescein in confocal laser scanning fluorescence microscopy. The parameters used for this simulation are: [F] = 10 mM, $[O_2]$ = 250 μM, $k_a = 3.8 \times 10^8\ s^{-1}$. (*a*) Population kinetics of fluorescein molecules in different energy states or the radical forms. (*b*) Kinetic curve of the ground state depletion, transformed in log. (*c*) Formation of the bleached dye molecules due to D-D and D-O mechanisms.

in solution where N_s was low and $N_s \ll N_{O_2}$, the build-up of the bleached molecules was primarily due to the D-O mechanism (Fig. 6). In the simulated microscopy, where N_s was high and $N_s/N_{O_2} > 0.2$, the bleached molecules were produced mainly from the D-D reactions (Fig. 9 *a*). When the D-D reactions were artificially suppressed, the bleached dye molecules were produced exclusively by the D-O reactions, and the kinetic curve of the singlet dye population was completely described by a single-exponential function (Fig. 9 *b*). This also suggests that the D-D reactions are the likely source of the deviation in the photobleaching behavior from a single-exponential function. Finally, when both D-D and D-O reactions are suppressed (and photobleaching is effectively inhibited), the populations of all the energy states move toward a steady state equilibrium, and remain so for $t \rightarrow \infty$ (Fig. 9 *d*).

Since the D-D mechanism involves more than one bimolecular reaction leading to the bleached dye molecules, the bleaching behavior will not be single exponential even in the absence of the D-O reactions. This is evident from Fig. 9 *c*. In the usual microscopy situation, the measurements are not carried out in the deoxygenated environment, and it is not reasonable to assume the absence of D-O reactions. Thus the photobleaching behavior is a composite effect of the simultaneous D-O and D-D reactions. The theoretical simulation, which bases itself on the photochemical and photophysical findings in Lindqvist's studies (Lindqvist, 1960; Kasche and Lindqvist, 1964), has not only independently supported the findings of Usui et al. (1965) on a switchover of the mechanism due to the relative concentrations of fluorescein and oxygen, but also explained the non-single-exponential photobleaching process of fluorescein in microscopy.

Probability of D-D reactions

The important link between the photobleaching of free fluorescein in solution and bound fluorescein in microscopy has been the interpretation of the findings of Usui et al. (1965) on mechanism switching in the context of the microscope situation. In the case of free fluorescein in solution, the D-D reactions are facilitated by the freely moving and diffusing fluorescein molecules. In the case of immobilized fluorescein in microscopy, the D-D reactions are solely due to the close proximity of fluorescein molecules. The probability of D-D reactions depends not only on the number of A or T bases (to which the fluorescein molecules are attached) from the specific sequence of DNA, or the amount of fluorescein-incorporated probes, but also on the compactness of the three-dimensional helical structure in a two-dimension-like space on the glass slide.

The strengths and weaknesses of the simulation

The mathematical simulation has provided some explanations to the non-single-exponential bleaching phenomenon in the fluorescence microscopy. As discussed above, it has led to some new insight into and understanding of the photobleaching process of fluorescein in microscopy. Nevertheless, some weaknesses of the simulation need to be noted.

First, because of the difficulty in making accurate measurements of the excitation irradiance, the k_a values are only estimates. Although the outcome of the simulation will not affect the characteristic trend of the bleaching process, the bleaching rate (k_b), which can be derived from the singlet-excited state kinetic curve, should not be used as a reference point for the experimentally obtained k_b values. Nevertheless, the ability to predict a trend of the photobleaching process under a given set of experimental parameters (i.e., excitation irradiance and fluorochrome concentration) satisfies the analytical purpose of the present study.

Second, the current simulation has not incorporated the effect of oxygen diffusion. As a result, the oxygen concentration decreases without replenishment as the reactions proceed. In practice, however, oxygen constantly diffuses toward the area of the lower O_2 partial pressure. A preliminary calculation (not shown) based on the diffusion of oxygen in aqueous medium indicates that in the usual conventional fluorescence microscopy with steady illumination using an arc lamp, the rate of the O_2 consumption by the photochemical reactions is unlikely to be faster than that of the O_2 diffusion from the environment. This calculation was tested in the simulation where N_{O_2} was made constant at $N_{O_2}(t = 0)$. The resultant kinetic curve of the singlet-excited state dye hardly differed from that of decreasing N_{O_2}.

Third, a further proof of the photobleaching mechanism in microscopy could be obtained by a photochemical approach in which the kinetics of transient fluorescein species, such as semi-reduced and semi-oxidized dye, are directly measured. However, such measurement is complicated by the short (transient) time domain and their very low absorption.

Finally, the analysis of the experimental results and the simulation did not assume an impurity in fluorescein. However, molecular heterogeneity, if present in sufficient amount, could further complicate the overall behavior of photobleaching.

The simulation in the current study remains a specific model for fluorescein only, since all the photochemical knowledge incorporated into the simulation is specific to fluorescein. However, reactions involving triplet dye molecules or a triplet and a ground state dye molecule are not unique to fluorescein. The general analytical approach used in the present study can be employed to study the photobleaching process of other common fluorochromes in biomedical microscopy, provided that sufficient knowledge of photochemical and photophysical properties of those fluorochromes is available.

Summary and concluding remarks

The present study has addressed a fundamental question about the photobleaching mechanism of fluorescein in microscopy. It has demonstrated through both experimental and theoretical methods that the single-exponential behavior is only a special case of the bleaching process when the average intermolecular distance of fluorescein is significantly greater than the average distance to oxygen, and that the photobleaching process of bound fluorescein in microscopy is in general not a single-exponential process. The improved understanding of photobleaching mechanism in microscopy will have a direct application in quantitation of fluorescence emission.

The authors would like to thank Dr. Tom M. Jovin (Max Planck Institute for Biophysical Chemistry, Göttingen, Germany) for his critical reading of this manuscript. The authors also wish to acknowledge the following persons for their contribution to or assistance in this study: Frans van der Rijke (Department of Cytochemistry and Cytometry, Leiden University) for the laboratory assistance and preparation of in situ hybridization of lymphocytes used in this study; Dr. Tom Dubbelman and Dr. Jolanda van der Zee (Department of Medical Biochemistry, Leiden University) for their many helpful discussions on photochemistry and the use of their laboratory facilities; Dr. C. A. G. O. Varma (Department of Organic Chemistry, Leiden University) for his interest in this work and useful discussions on photophysics.

REFERENCES

Axelrod, D., D. E. Koppel, J. Schlessinger, E. Elson, and W. W. Webb. 1976. Mobility measurement by analysis of fluorescence photobleaching recovery kinetics. *Biophys. J.* 16:1055–1069.

Benson, D. M., J. Bryan, A. L. Plant, A. M. Gotto, Jr., and L. C. Smith. 1985. Digital imaging fluorescence microscopy: spatial heterogeneity of photobleaching rate constants in individual cells. *J. Cell Biol.* 100: 1309–1323.

Carrington, W. A., K. E. Fogarty, L. Lifschitz, and F. S. Fay. 1989. Three-dimensional imaging on confocal and wide-field microscopes. *In* The Handbook for Biological Confocal Microscopy. J. Pawley, editor. IMR Press, Madison, Wisconsin.

Edidin, M., Y. Zagyansky, and T. J. Lardner. 1976. Measurement of membrane protein lateral diffusion in single cells. *Science.* 191:466–468.

Gollnick, K., T. Franken, M. F. R. Fouda, H. R. Paur, and S. Held. 1992. Merbromin (mercurochrome) and other xanthene dyes: quantum yields of triplet sensitizer generation and singlet oxygen formation in alcoholic solutions. *J. Photochem. Photobiol. B: Biol.* 12:57–81.

Hindmarsh, A. C. 1983. ODEPACK, a systematized collection of ODE solvers. *In* Scientific Computing. R. S. Stepleman, editor. North-Holland, Amsterdam. 55–64.

Hirschfeld, T. 1976. Quantum efficiency independence of the time integrated emission from a fluorescent molecule. *Appl. Opt.* 15:3135–3139.

Imamura, M. and M. Koizumi. 1955. Irreversible photobleaching of the solution of fluorescent dyes. I. Kinetic studies on the primary process. *Bull. Chem. Soc. Jpn.* 28:117–124.

Jacobson, K., E.-S. Wu, and G. Poste. 1976. Measurement of the translational mobility of concanavalin A in glycerol-saline solutions and on the cell surface by fluorescence recovery after photobleaching. *Biochim. Biophys. Acta.* 423:215–222.

Johnson, G. D., R. S. Davidson, K. C. McNamee, G. Russell, D. Goodwin, and E. J. Holborow. 1982. Fading of immunofluorescence during microscopy: a study of the phenomenon and its remedy. *J. Immunol Methods.* 55:231–242.

Jovin, T. M., and D. J. Arndt-Jovin. 1989. FRET microscopy: digital imaging of fluorescence resonance energy transfer. Application in cell biology. *In* Cell Structure and Function by Microspectrofluorometry. E. Kohen and J. G. Hirschberg, editors. Academic Press, Inc., London. 99–117.

Jovin, T. M., D. J. Arndt-Jovin, G. Marriott, R. M. Clegg, M. Robert-Nicoud, and T. Schormann. 1990. Distance, wavelength and time: the versatile 3rd dimensions in light emission microscopy. *In* Optical Microscopy for Biology. B. Herman and K. Jacobson, editors. Wiley-Liss, Inc., New York. 575–602.

Kasche, V., and L. Lindqvist. 1964. Reactions between the triplet state of fluorescein and oxygen. *J. Phys. Chem.* 68:817–823.

Koppel, D. E., C. Carlson, and H. Smilowitz. 1989. Analysis of heterogeneous fluorescence photobleaching by video kinetics imaging: the method of cumulants. *J. Microsc.* 155:199–206.

Koppel, D. E., P. Primakoff, and D. G. Myles. 1986. Fluorescence photobleaching analysis of cell surface regionalization. *In* Applications of Fluorescence in the Biomedical Sciences. D. L. Taylor, A. S. Waggoner, R. F. Murphy, F. Lanni, and R. Birge, editors. Alan R Liss, Inc., New York. 477–497.

Krüger, U., and R. Memming. 1974. Formation and reactions of long lived xanthene dye radicals. I. Photochemical studies on reactions of semireduced fluorescein. *Berichte der Bunsen-Gesellschaft.* 78:670–678.

Kubitscheck, U., M. Kircheis, R. Schweitzer-Stenner, W. Dreybrodt, T. M. Jovin, and I. Pecht. 1991. Fluorescence resonance energy transfer on single living cells. Application to binding of monovalent haptens to cell-bound immunoglobulin E. *Biophys. J.* 60:307–318.

Kubitscheck, U., R. Schweitzer-Stenner, D. J. Arndt-Jovin, T. M. Jovin, and I. Pecht. 1993. Distribution of type I Fc-receptors on the surface of mast cells probed by fluorescence resonance energy transfer. *Biophys. J.* 64: 110–120.

Lindqvist, L. 1960. A flash photolysis study of fluorescein. *Arkiv för Kemi.* 16:79–138.

Marriott, G., R. M. Clegg, D. J. Arndt-Jovin, and T. M. Jovin. 1991. Time resolved imaging microscopy. Phosphorescence and delayed fluorescence. *Biophys. J.* 60:1374–1387.

Peters, R., A. Brünger, and K. Schulten. 1981. Continuous fluorescence microphotolysis: a sensitive method for study of diffusion processes in single cells. *Proc. Natl. Acad. Sci. USA.* 78:962–966.

Peters, R., J. Peters, K. H. Tews, and W. Bahr. 1974. Microfluorimetric study of translational diffusion of proteins in erythrocyte-membrane. *Biochim. Biophys. Acta.* 367:282–294.

Press, W. H., S. A. Keukolsky, W. T. Vetterling, and B. P. Flannery. 1992. Numerical Recipes in C: The Art of Scientific Computing. Cambridge University Press, Cambridge.

Rigaut, J. P., and J. Vassy. 1991. High-resolution three-dimensional images from confocal scanning laser microscopy. Quantitative study and mathematical correction of the effects from bleaching and fluorescence attenuation in depth. *Anal. Quant. Cytol. Histol.* 13:223–232.

Schlessinger, J., D. Axelrod, D. E. Koppel, W. W. Webb, and E. L. Elson. 1977. Lateral transport of a lipid probe and labeled proteins on a cell-membrane. *Science.* 195:307–309.

Schlessinger, J., D. E. Koppel, D. Axelrod, K. Jacobson, W. W. Webb, and E. L. Elson. 1976. Lateral transport on cell membranes: mobility of concanavalin A receptors on myoblasts. *Proc. Natl. Acad. Sci. USA.* 73: 2409–2413.

Szabò, G., Jr., P. S. Pine, J. L. Weaver, M. Kasari, and A. Aszalos. 1992. Epitope mapping by photobleaching fluorescence resonance energy transfer measurements using a laser scanning microscope system. *Biophys. J.* 61:661–670.

Tsien, R. Y., and A. Waggoner. 1989. Fluorophores for confocal microscopy: photophysics and photochemistry. *In* The Handbook for Biological Confocal Microscopy. J. Pawley, editor. IMR Press, Madison, Wisconsin. 153–161.

Usui, Y., K. Itoh, and M. Koizumi. 1965. Switch-over of the mechanism of the primary processes in the photo-oxidation of xanthene dyes as revealed by the oxygen consumption experiments. *Bull. Chem. Soc. Jpn.* 38:1015–1022.

Vaughan, W. M., and G. Weber. 1970. Oxygen quenching of pyrenebutyric acid fluorescence in water. A dynamic probe of the microenvironment. *Biochemistry.* 9:464–473.

Wells, K. S., D. R. Sandison, J. Strickler, and W. W. Webb. 1989. Quantitative fluorescence imaging with laser scanning confocal microscopy. *In* The Handbook for Biological Confocal Microscopy. J. Pawley, editor. IMR Press, Madison, Wisconsin.

Young, R. M., J. K. Arnette, D. A. Roess, and B. G. Barisas. 1994. Quantitation of fluorescence energy transfer between cell surface proteins via fluorescence donor photobleaching kinetics. *Biophys. J.* 67:881–888.